Genetic Responses to Nanostructured Calcium-phosphate-coated Implants

R. Jimbo, Y. Xue, M. Hayashi, H. O. Schwartz-Filho, M. Andersson, K. Mustafa and A. Wennerberg

J DENT RES published online 20 September 2011
DOI: 10.1177/0022034511422911

RESEARCH REPORTS
Biomaterials & Bioengineering

R. Jimbo[1]*, Y. Xue[2], M. Hayashi[1], H.O. Schwartz-Filho[1,3], M. Andersson[4], K. Mustafa[2], and A. Wennerberg[1]

[1]Surface Biology Group, Department of Prosthodontics, Faculty of Odontology, Malmö University, 205 06 Malmö, Sweden; [2]Department of Clinical Dentistry, Center for Clinical Dental Research, University of Bergen, Norway; [3]Division of Periodontology, Department of Oral Diagnosis and Surgery, School of Dentistry, UNESP, São Paulo State University, Araraquara, SP, Brazil; and [4]Department of Chemical and Biological Engineering, Applied Surface Chemistry, Chalmers University of Technology, Gothenburg, Sweden; *corresponding author, ryo.jimbo@mah.se

J Dent Res X(X):xx-xx, XXXX

Genetic Responses to Nanostructured Calcium-phosphate-coated Implants

ABSTRACT

Nanostructured calcium phosphate (CaP) has been histologically and biomechanically proven to enhance osseointegration of implants; however, conventional techniques were not sufficiently sensitive to capture its biological effects fully. Here, we compared the conventional removal torque (RTQ) evaluation and gene expression in tissues around nanostructured CaP-coated implants, using real-time RT-PCR, with those of uncoated implants, in a rabbit model. At 2 wks, RTQ values were significantly higher, alkaline phosphatase (ALP) expression was significantly higher, and runt-related transcription factor 2 and tumor necrosis factor-α expressions were significantly lower in the coated than in the uncoated implants. This indicates that inflammatory responses were suppressed and osteoprogenitor activity increased around the CaP-coated surface. At 4 wks, although RTQ values did not significantly differ between the 2 groups, ALP and osteocalcin (OCN) were significantly up-regulated in the coated group, indicating progressive mineralization of the bone around the implant. Moreover, an osteoclast marker, adenosine triphosphatase, which indicates acidification of the resorption lacunae, was significantly higher for the coated implants, suggesting gradual resorption of the CaP coating. This study reveals detailed genetic responses to nanostructured CaP-coated implants and provides evidence that the effect of nanotopography is significant during the osseointegration cascade.

KEY WORDS: gene expression, biomaterials, nanotopography, bone implant interactions, osseointegration, calcium phosphate coating.

DOI: 10.1177/0022034511422911

Received July 8, 2011; Revised August 18, 2011; Accepted August 18, 2011

INTRODUCTION

The application of nanotopography to implant surfaces, currently considered cutting-edge research, has proven to significantly enhance osseointegration (Wennerberg and Albrektsson, 2010). Recent *in vivo* studies have shown that nanostructured implant surfaces enhance bone responses, as measured both histologically and biomechanically (Bjursten *et al*., 2010; Jimbo *et al.*, 2011b). The beneficial effects of these alterations may stem from conversion of the material to a highly bioactive state because of modifications at the nano level (Goransson *et al.*, 2006; Frojd *et al.*, 2011), which is the core concept of the biologically inspired biomimetic engineering (Flammang and Porter, 2011).

Nano-scale roughness may well be the decisive factor for osteogenesis, because the size of proteins and cell membrane receptors corresponds to surface topography on this length scale. Gittens *et al.* (2011) reported that nano-scale modifications considerably enhanced the differentiation of pre-osteoblasts, which showed significantly higher levels of osteocalcin and osteoprotegerin expression *in vitro* (Gittens *et al.,* 2011). In another study, the titanium surfaces of implants were modified with H_2SO_4/H_2O_2, and it was reported that the modified nanostructured surface up-regulated bone-specific gene expression in human mesenchymal stem cells in culture (Mendonca *et al.*, 2010). Moreover, the effect of nanotopography has been reported to modify cellular shape, which influences cell fate, *e.g*., apoptosis, growth, and differentiation (Huang and Ingber, 2000).

Among the numerous nano-modification methods, the deposition of nano-sized calcium phosphate (CaP) coatings seems to be an interesting modification, because it has been reported to mimic the composition and structure of the surrounding bone (Liao *et al*., 2004). Here, the synergistic effect of both bone-like chemistry and topography may trigger cellular responses that contribute to accelerated bone responses (Wennerberg and Albrektsson, 2011; Mendonca *et al.*, 2010; Gittens *et al.,* 2011).

Although *in vitro* studies suggest that nano-sized CaP coatings are a promising modification, *in vivo* results have not consistently indicated significant benefits (Svanborg *et al.*, 2010). This may be because most of the evaluation techniques, such as the biomechanical evaluation with removal torque, are fairly coarse and may not fully capture the sensitive effect of the nano-level modification; thus, further detailed evaluation of this modification is required. Hence, in this study, we used real-time reverse transcription (RT-PCR) for the first time in rabbits to investigate genetic responses to nanostructured CaP coating of implants, as a complement to conventional removal torque analysis, to

Table. Designed Oligonucleotide Sequences of Sense (S) and Antisense (A) Primers Used in the Real-time RT-PCR of Target and Housekeeping Genes

Gene		Primer Sequence	T_m Amplicon (C°)	Amplicon Size (bp)	Primer Source
ALP	S	5′-TGGACCTCGTGGACATCTG-3′	75	80	*Oryctolagus cuniculus*
	A	5′-CAGGAGTTCAGTGCGGTTC-3′			
ATPase	S	5′-CCTGGCTATTGGCTGTTACG-3′	77.7	98	*Oryctolagus cuniculus*
	A	5′-GCTGGTAGAAGGACACTCTTG-3′			
Calcitonin receptor	S	5′-CGTTCACTCCTGAAAACTACA-3′	72.6	128	*Oryctolagus cuniculus*
	A	5′-GCAACCAAGACTAATGAAACA-3′			
Collagen-I	S	5′-GGAAACGATGGTGCTACTGG-3′	80.4	83	*Oryctolagus cuniculus*
	A	5′-CCGACAGCTCCAGGGAAG-3′			
IGF-1	S	5′-CCGACATGCCCAAGACTCA-3′	70.3	81	*Oryctolagus cuniculus*
	A	5′-TACTTCCTTTCCTTCTCCTCTGA-3′			
IL-6	S	5′-GAGGAAAGAGATGTGTGACCAT-3′	73.5	104	*Oryctolagus cuniculus*
	A	5′-AGCATCCGTCTTCTTCTATCAG-3′			
Osteocalcin	S	5′-GCTCAHCCTTCGTGTCCAAG-3′	77.8	70	*Oryctolagus cuniculus*
	A	5′-CCGTCGATCAGTTGGCGC-3′			
RUNX-2	S	5′-GCAGTTCCCAAGCATTTCATC-3′	72.8	81	*Oryctolagus cuniculus*
	A	5′-GTGTAAGTAAAGGTGGCTGGATA-3′			
TNF-α	S	5′-CTCACTACTCCCAGGTTCTCT-3′	78.2	122	*Oryctolagus cuniculus*
	A	5′-TTGATGGCAGAGAGGAGGTT-3′			
TRAP	S	5′-GCTACCTCCGCTTCCACTA-3′	78.5	129	*Oryctolagus cuniculus*
	A	5′-GCAGCCTGGTCTTGAAGAG-3′			
β-actin	S	5′-CACCCTGATGCTCAAGTACC-3′	76.4	96	*Oryctolagus cuniculus*
	A	5′-CGCAGCTCGTTGTAGAAGG-3′			

further clarify the effects of CaP-coating on osseointegration. In the hope of observing the osteogenesis, osteoclastogenesis, and inflammatory responses, we selected a total of 10 genes for the analysis. We were interested in observing osseointegration multi-directionally, since we hypothesized that the nanostructured CaP coating would have significant effects not only on osteogenesis but also on both osteoclastogenesis and inflammatory reactions.

MATERIALS & METHODS

Implant Surface Preparation and Characterization

Thirty-six threaded implants, prepared from commercially pure titanium (Grade 4), of 8 mm length and 3.3 mm diameter were used. Half of the implants (test) were coated with nano-sized CaP according to the Promimic $HA^{NANO™}$ method, as described in more detail elsewhere (Kjellin and Andersson, 2006). Briefly, the implants were dipped in a CaP-nanoparticle dispersion, followed by heat treatment at 550°C for 5 min in an oxygen atmosphere. The CaP nanoparticle dispersion was stabilized (*i.e.,* when sedimentation or precipitation of the particles is prevented) by electrostatic nanoparticle stabilization at pH = 9, as well as by steric stabilization, through the addition of surfactants. The other half of the implants remained uncoated but were subjected to a heat treatment in the same manner as the test implants (control).

Scanning Electron Microscopy

Surface morphology of the implants was examined by scanning electron microscopy (SEM) with LEO Ultra 55 FEG (Zeiss, Oberkochen, Germany) at an accelerating voltage of 6 kV. Three randomly selected implants from each group were investigated.

Interferometry

Surface topography was characterized by means of an interferometer (MicroXam; ADE Phase Shift, Inc., Tucson, AZ, USA). Three implants from each group were randomly selected and each investigated in 9 regions (3 top regions, 3 thread valleys, and 3 flank regions). The parametric calculation was performed after the removal of errors of form and waviness by the use of a 50 × 50 μm Gaussian filter. The following 3D parameters were selected: S_a (μm) = the arithmetic average height deviation from a mean plane; S_{ds} (μm^{-2}) = the density of summits; and S_{dr} (%) = the developed surface ratio.

Animals, Implantation, and Sample Preparation

The animal study was approved by the Malmö/Lund, Sweden, regional animal ethics committee (approval number: M282-09).

One test implant and one control implant were inserted into the left and right tibia, respectively, of 18 lop-eared rabbits (mean body weight, 3.9 kg). Before surgery, the hind legs were shaved and disinfected with 70% ethanol and 70% chlorhexidine. The animals were anesthetized with intramuscular injections of a mixture of 0.15 mL/kg medetomidine (1 mg/mL Dormitor; Orion Pharma, Sollentuna, Sweden) and 0.35 mL/kg ketamine hydrochloride (50 mg/mL Ketalar; Pfizer AB, Sollentuna, Sweden). Lidocaine hydrochloride (Xylocaine; AstraZeneca AB, Södertälje, Sweden) was administered as the local anesthetic at each insertion site at a dose of 1 mL. The

implants were inserted with a W&H implant unit (Elcomed, W&H SA-310, Burmoos, Austria) with the rotation speed set at 20 revolutions *per* min. During implant placement, the insertion torque (ITQ) was measured and recorded by the drilling unit throughout the installation procedure. Post-operatively, buprenorphine hydrochloride (0.5 mL Temgesic; Reckitt Benckiser, Slough, UK) was administered as an analgesic for 3 days.

Insertion Torque and Removal Torque Analysis

After 2 and 4 wks, the rabbits were sacrificed (n = 9 for each time-point) with an overdose (60 mg/mL) of pentobarbitalnatrium (Apoteksbolaget AB, Stockholm, Sweden). The skin above the implants was incised, and the force necessary to unscrew the implants was immediately measured with the use of a Tohnichi 6 BTG-N instrument (Tohnichi MFG, Ota-Ku, Japan) with a measuring range from 0 to 74 Ncm. The highest values were recorded as the removal torque (RTQ) values.

RNA Extraction and Real-time Reverse-transcription PCR

After the RTQ test, the removal torqued implants and the surrounding tissues were carefully collected with the use of a Φ4.4 mm trephine bur (GC Dental, Tokyo, Japan); thereafter, the samples were placed in RNA*later* solution (QIAGEN GmbH, Hilden, Germany), and frozen at -80°C until analysis. For both groups, total RNA was isolated from the tissue specimens with Trizol® reagent (Gibco BRL, Carlsbad, CA, USA) combined with E.Z.N.A.™ Tissue RNA isolation kit (Omega Bio-Tek, Norcross, GA, USA), and quantified by means of a NanoDrop Spectrophotometer (ThermoScientific NanoDrop Technologies, Wilmington, DE, USA).

Reverse transcription was performed on 6 ng/μL of the total RNA, with the High Capacity cDNA Archive Kit (Applied Biosystems, Foster City, CA, USA) according to the manufacturer's instructions.

Real-time quantitative reverse transcription (RT-PCR) was performed in 20-μL volumes, and in triplicate for each target cDNA, with standard enzyme and cycling conditions on a 96-well StepOne™ system (Applied Biosystems), with custom-designed real-time assays and SYBR® green detection (PrimerDesign Ltd, Southampton, UK) (Table). cDNA corresponding to 10 ng of mRNA was used as template in each PCR reaction.

As an endogenous control, levels of β-actin were quantified in parallel with target genes. Normalization and fold-changes were calculated with StepOne™ software with the ΔΔCt method (Schmittgen and Livak, 2008).

Statistical Analysis

Statistical analyses were performed with KaleidaGraph software (Synergy Software; Essex Junction, VT, USA). Topography, interferometry, and torque data are given as mean (SD). The mean values of surface roughness were compared by one-way ANOVA, followed by a *post hoc* Tukey-Kramer test. A non-parametric Wilcoxon signed-rank test was used for bilaterally inserted implants. For gene expression analysis, Student's paired *t* test was used to compare the 2 groups. Any p values less than 0.05 were considered significant.

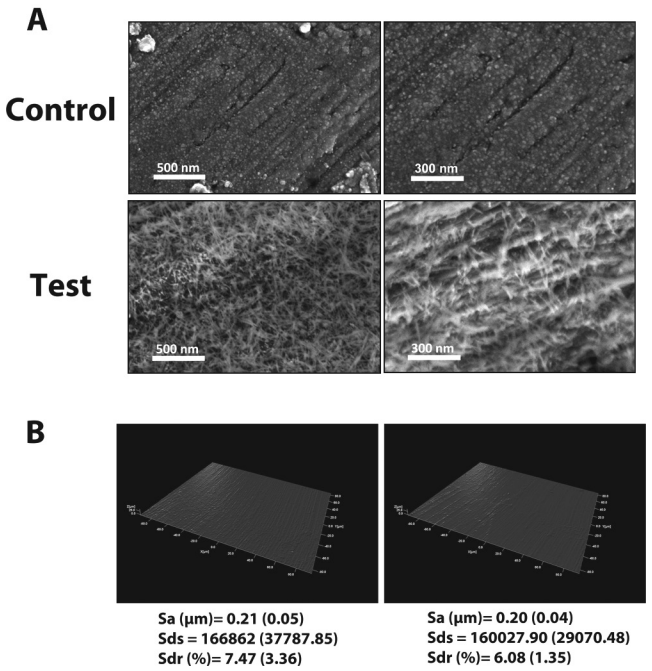

Figure 1. Implant surface characterization by scanning electron microscopy and interferometry. Oxide formation was found on the heat-treated (control) surface for both magnifications. Whereas the nano CaP-coated surface (test) was fully covered with needle-shaped nanoparticles, it can be seen, on the further magnified image of the test surface, that each needle is approximately 10 to 20 nm in width and 100 to 200 nm in length. The 3D reconstructed images of the control and test surfaces and the corresponding surface roughness measurements (Sa, Sds, and Sdr) show that no significant differences at the micro level could be detected between the 2 groups.

RESULTS

Calcium Phosphate Nano-crystalline Topography

SEM images of both the test and control implants are presented in Fig. 1A. At high magnification, it is evident that the implant surface was fully covered with rod-shaped CaP particles of a size approximately 10 to 20 nm in width and 100 to 200 nm in length, whereas the heat-treated control presented spherical structures on the surface.

Fig. 1B presents 3D optical interferometry images of the control and test surfaces, respectively. The mean S_a value was 0.21 (0.05) and 0.20 (0.04) for the control and test implants, respectively. The mean S_{ds} was 166862 (37787.85) and 160027.90 (29070.48) for the control and test implants, respectively. The mean S_{dr} percentage was 7.47 (3.36) and 6.08 (1.35) for the control and test implants, respectively. There were no significant differences between the compared parameters.

Insertion Torque and Removal Torque Analysis

The results of the insertion torque and removal torque tests are presented in Fig. 2. Significant differences in insertion torque between the control and test implants were not observed at either 2 or 4 wks. The mean removal torque values differed significantly (p = 0.01187) between the control (8.8 [2.4]) and

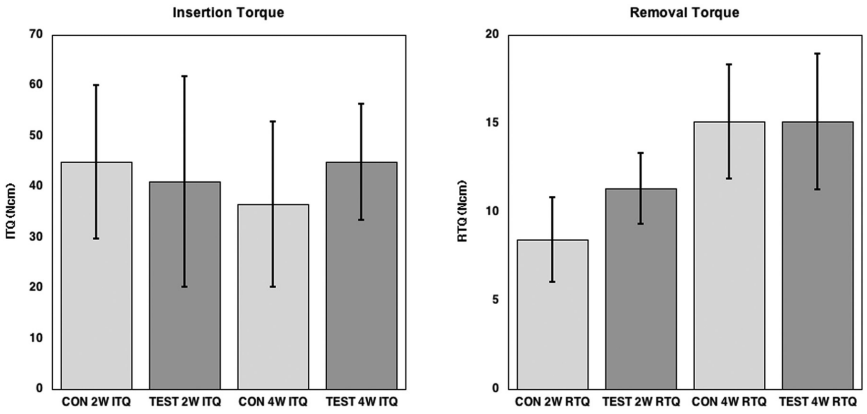

Figure 2. Graph showing the insertion torque (ITQ) and removal torque (RTQ) results. No statistically significant differences could be seen for the ITQ. The RTQ value at 2 wks showed statistically higher RTQ for the test surface, whereas at 4 wks, no significant differences could be seen between the 2 groups.

test (11.9 [1.7]) implants at 2 wks, but not at 4 wks (control, 15.5 [3.2]; test, 15.1 [4.1]).

Gene Expression

The RT-PCR results are presented in Figs. 3A and 3B. At 2 wks, the expression of ALP at the test surface (0.976 [1.223]) was significantly higher than that at the control surface (0.439 [0.547]) (2.22-fold, $p < 0.05$), whereas the expressions of RUNX-2 and TNF-α were significantly lower for the test (0.285 [0.148] and 0.531 [0.349], respectively) than the control samples (0.342 [0.132] and 0.606 [0.217], respectively) (RUNX-2, 0.52-fold, $p < 0.05$; and TNF-α, 0.56-fold, $p < 0.01$).

At 4 wks, the expression of ALP, osteocalcin, and ATPase was significantly higher for the test samples (151.504 [226.197], 4.341 [10.417], and 2268.212 [3014.843], respectively) than for the control samples (4.717 [4.490], 1.055 [0.392], and 0.757 [0.224], respectively) (ALP, 34.9-fold, $p < 0.05$; osteocalcin, 480-fold, $p < 0.05$; and ATPase, 1.39-fold, $p < 0.05$). No statistically significant differences could be observed for the other markers tested.

DISCUSSION

This study investigates the detailed genetic responses to nanostructured implants in a rabbit model. Although most of the previous *in vivo* studies on the effect of nanotopography have been conducted in rabbits, the results from this present study shed light on the heretofore unknown interactions occurring at the bone-to-implant interface, which cannot be distinguished by conventional techniques. Indeed, an important aim of the present study was to reveal molecular processes that underlie the observed biomechanics, by combining information obtained from biomechanical testing with that obtained from gene expression analysis. Based on the previously reported histological and biomechanical studies (Bjursten *et al.,* 2010; Jimbo *et al.*, 2011a), it is suggested that the effect of nanotopography in terms of bone acceleration occurs early. Therefore, in this study, we focused on the genetic responses at 2 and 4 wks, which is a commonly used time frame to evaluate initial osseointegration.

Nano-sized CaP-coated implants showed significantly higher RTQ values compared with uncoated implants at 2 wks, whereas at 4 wks, no significant differences were found between the implants, indicating that the nanostructured CaP coating enhanced the initial bone responses.

In contrast, clear differences in osteogenic gene expression were observed for CaP-coated implants, compared with non-coated implants, at both 2 and 4 wks. At 2 wks, the tissue surrounding the nanostructured CaP-coated surface showed significantly higher expression of ALP than did the tissue around the non-coated control surface. This indicates that the modified surface promoted higher osteoprogenitor activity (Pinzone *et al.,* 2009), and is an indication that early bone formation was significant around this surface. This finding is in accordance with the results of the study conducted by Masaki *et al.,* who showed that ALP expression increased when cultured mesenchymal cells were exposed to different surface topographies, which was suggested to be attributed to the morphologic alteration caused by a specific surface topography (Masaki *et al*., 2005).

At 4 wks, the expression levels of both ALP and osteocalcin were significantly higher for the test implants than for the control implants; similarly, expression of collagen type I was also higher for the test than for the control implants, although the difference did not reach statistical significance. Because osteocalcin is a strong indicator of osteoblast differentiation (Yonezawa *et al*., 2011), and temporal expression and maturation of extracellular matrix proteins such as fibronectin (Jimbo *et al.*, 2007) or collagen type I (Franceschi and Iyer, 1992; Jimbo *et al.*, 2010) are essential for mineralization, these results indicate that the rate of mineralization was enhanced for the test implants.

Interestingly, at 2 wks, the expression of RUNX-2 was significantly lower for the coated implants than for the control implants. Because RUNX-2 is known to be a transcription factor indispensable for osteoblast differentiation and functions upstream to osterix (Ma *et al.*, 2011) and osteocalcin (Pinzone *et al*., 2009), increased expression of ALP could be expected to induce increased expression of RUNX-2. However, the approximately 60% lower expression of RUNX-2 in the present study by 2 wks suggests that the 2 factors are regulated by different signaling pathways. Furthermore, the reduced expression of RUNX-2 after 2 wks hints at the presence of a negative feedback mechanism that controls the RUNX-2 expression on the test samples after its maximum expression, which might occur at an earlier time-point. However, since we investigated only 2 time-points, the study design precluded evaluation of the dynamic RUNX-2 in response to the different types of surfaces.

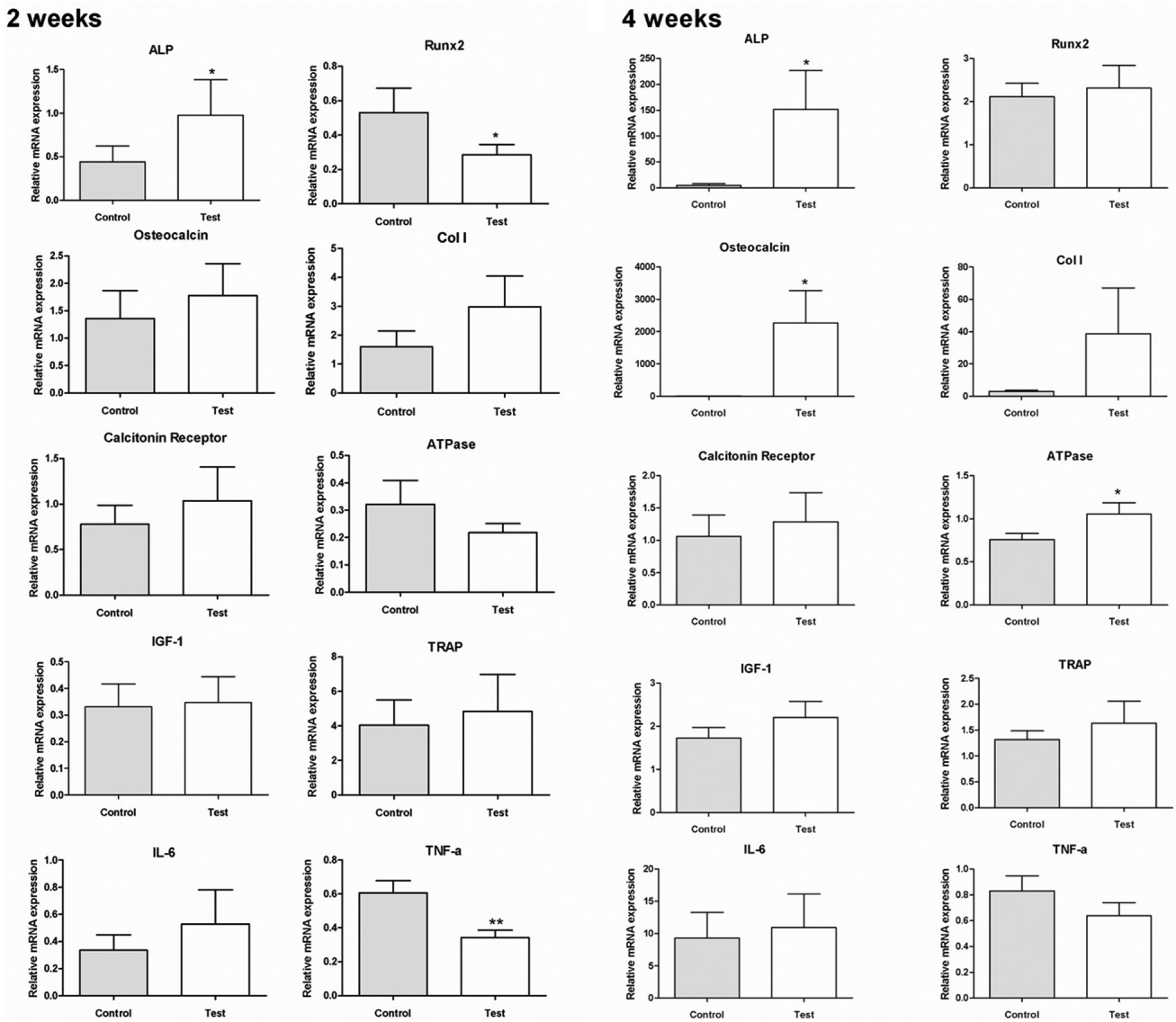

Figure 3. Gene expressions of selected markers quantified by real-time RT-PCR. After 2 wks and 4 wks, the removal torqued implants and the surrounding tissue were collected, and total RNA of samples was isolated (n = 9 for each time-point). The osteogenic markers (ALP, osteocalcin, Runx2, calcitonin receptor, collagen I, TRAP, IGF-1, and ATPase) and inflammation markers (IL-6 and TNF-α) were analyzed. The relative expressions of target genes were normalized with the housekeeping gene β-actin (*$p < 0.05$ and **$p < 0.01$).

This is also in accordance with *in vitro* data from a study by Masaki *et al.* (2005), who showed that ALP and RUNX-2 expression levels can be opposite and suggested that different intracellular signaling pathways regulate the expression of these 2 genes in response to implant surface microtopography (Masaki *et al.,* 2005). Because the surface roughness parameters at the micro level showed no differences in the present study, we suggest that nanotopography is the decisive factor that affects the expression of these early bone formation markers.

Furthermore, inflammatory responses to the control and test surfaces seemed to differ. The expression level of TNF-α was significantly lower for the test samples than for the control samples. TNF-α has been reported to be a predominant pro-inflammatory mediator of bone loss (Cenci *et al.*, 2000); it inhibits osteoblast activity and bone mineralization by down-regulating growth factors such as IGF-I and ALP (Gilbert *et al*., 2000). TNF-α also alters osteoblast signaling by increasing RANKL production (Wei *et al.*, 2005) and accelerates osteoclastogenesis (Bu *et al*., 2009). Dimitrievska *et al.* (2008) reported that the presence of hydroxyapatite in nanocomposite fiber scaffolds significantly decreased TNF-α expression and enhanced the biocompatibility of the fibers. Hence, the nanostructured CaP-coating may have suppressed the inflammatory response at 2 wks, and thus enhanced the ALP expression.

At 4 wks, expression of an osteoclast marker, *i.e*., ATPase, was notably higher in the test group. Acidification of the resorption lacuna has been shown to be mediated by the vacuolar class of ATP-driven proton pump (H +-ATPase), which is located in

the osteoclast-ruffled border (Kelly *et al.*, 1992). A possible explanation for the significantly higher expression of ATPase could be that resorption of the CaP monolayer coating may have commenced after 4 wks. However, previous studies have indicated that osteoclast function is eventually suppressed during this process, and recrystallization is subsequently provoked by high calcium ion concentrations (Leeuwenburgh *et al.*, 2001). Hence, it can be speculated that the gradual resorption of the CaP-coating had no significant effect on biomechanics by 4 wks, because the progressive osteoblastogenesis had more than compensated for the resorption of the CaP-coating by constantly forming and mineralizing bone.

Many implant manufacturers have applied nanostructures to their implant surfaces with the hope of increasing bone apposition to the implant surfaces, but they lacked strong corroborating evidence. In this study, the combination of gene expression and conventional biomechanical evaluation not only provided evidence that a nanostructured CaP-coated surface enhances osteointegration, but also revealed distinct biochemical responses to the coating that underlie the increased osteogenesis, which could not have been observed through the use of conventional techniques.

ACKNOWLEDGMENTS

This study was supported by the Swedish Knowledge Foundation, the Swedish Research Council, and the Hjalmar Svensson Research Foundation. The authors thank Dr. Kazuo Hirota of GC Dental for his kind support. The authors declare no potential conflicts of interest with respect to the authorship and/or publication of this article.

REFERENCES

Bjursten LM, Rasmusson L, Oh S, Smith GC, Brammer KS, Jin S (2010). Titanium dioxide nanotubes enhance bone bonding in vivo. *J Biomed Mater Res A* 92:1218-1224.

Bu SY, Hunt TS, Smith BJ (2009). Dried plum polyphenols attenuate the detrimental effects of TNF-alpha on osteoblast function coincident with up-regulation of Runx2, Osterix and IGF-I. *J Nutr Biochem* 20:35-44.

Cenci S, Weitzmann MN, Roggia C, Namba N, Novack D, Woodring J, *et al.* (2000). Estrogen deficiency induces bone loss by enhancing T-cell production of TNF-alpha. *J Clin Invest* 106:1229-1237.

Dimitrievska S, Petit A, Ajji A, Bureau MN, Yahia L (2008). Biocompatibility of novel polymer-apatite nanocomposite fibers. *J Biomed Mater Res A* 84:44-53.

Flammang BE, Porter ME (2011). Bioinspiration: applying mechanical design to experimental biology. *Integr Comp Biol* 51:128-132.

Franceschi RT, Iyer BS (1992). Relationship between collagen synthesis and expression of the osteoblast phenotype in MC3T3-E1 cells. *J Bone Miner Res* 7:235-246.

Frojd V, Wennerberg A, Franke Stenport V (2011). Importance of Ca(2+) modifications for osseointegration of smooth and moderately rough anodized titanium implants—a removal torque and histological evaluation in rabbit. *Clin Implant Dent Relat Res* [Epub ahead of print, Oct 26, 2011] (in press).

Gilbert L, He X, Farmer P, Boden S, Kozlowski M, Rubin J, *et al.* (2000). Inhibition of osteoblast differentiation by tumor necrosis factor-alpha. *Endocrinology* 141:3956-3964.

Gittens RA, McLachlan T, Olivares-Navarrete R, Cai Y, Berner S, Tannenbaum R, *et al.* (2011). The effects of combined micron-/submicron-scale surface roughness and nanoscale features on cell proliferation and differentiation. *Biomaterials* 32:3395-3403.

Goransson A, Gretzer C, Johansson A, Sul YT, Wennerberg A (2006). Inflammatory response to a titanium surface with potential bioactive properties: an in vitro study. *Clin Implant Dent Relat Res* 8:210-217.

Huang S, Ingber DE (2000). Shape-dependent control of cell growth, differentiation, and apoptosis: switching between attractors in cell regulatory networks. *Exp Cell Res* 261:91-103.

Jimbo R, Sawase T, Shibata Y, Hirata K, Hishikawa Y, Tanaka Y, *et al.* (2007). Enhanced osseointegration by the chemotactic activity of plasma fibronectin for cellular fibronectin positive cells. *Biomaterials* 28:3469-3477.

Jimbo R, Ivarsson M, Koskela A, Sul YT, Johansson CB (2010). Protein adsorption to surface chemistry and crystal structure modification of titanium surfaces. *J Oral Maxillofac Res* 1(3):e3.

Jimbo R, Coelho PG, Vandeweghe S, Schwartz-Filho HO, Hayashi M, Ono D, *et al.* (2011a). Histological and three-dimensional evaluation of osseointegration to nanostructured calcium phosphate-coated implants. *Acta Biomater* [Epub ahead of print July 21, 2011] (in press).

Jimbo R, Sotres J, Johansson C, Breding K, Currie F, Wennerberg A (2011b). The biological response to three different nanostructures applied on smooth implant surfaces. *Clin Oral Implants Res* [Epub ahead of print April 13, 2011] (in press).

Kelly ME, Dixon SJ, Sims SM (1992). Inwardly rectifying potassium current in rabbit osteoclasts: a whole-cell and single-channel study. *J Membr Biol* 126:171-181.

Kjellin P, Andersson M, inventors (2006). Synthetic nano-sized crystalline calcium phosphate and method of production. Patent SE527610. April 25.

Leeuwenburgh S, Layrolle P, Barrere F, de Bruijn J, Schoonman J, van Blitterswijk CA, *et al.* (2001). Osteoclastic resorption of biomimetic calcium phosphate coatings in vitro. *J Biomed Mater Res* 56:208-215.

Liao SS, Cui FZ, Zhang W, Feng QL (2004). Hierarchically biomimetic bone scaffold materials: nano-HA/collagen/PLA composite. *J Biomed Mater Res B Appl Biomater* 69:158-165.

Ma HP, Ming LG, Ge BF, Zhai YK, Song P, Xian CJ, *et al.* (2011). Icariin is more potent than genistein in promoting osteoblast differentiation and mineralization in vitro. *J Cell Biochem* 112:916-923.

Masaki C, Schneider GB, Zaharias R, Seabold D, Stanford C (2005). Effects of implant surface microtopography on osteoblast gene expression. *Clin Oral Implants Res* 16:650-656.

Mendonca G, Mendonca DB, Aragao FJ, Cooper LF (2010). The combination of micron and nanotopography by H(2)SO(4)/H(2)O(2) treatment and its effects on osteoblast-specific gene expression of hMSCs. *J Biomed Mater Res A* 94:169-179.

Pinzone JJ, Hall BM, Thudi NK, Vonau M, Qiang YW, Rosol TJ, *et al.* (2009). The role of Dickkopf-1 in bone development, homeostasis, and disease. *Blood* 113:517-525.

Schmittgen TD, Livak KJ (2008). Analyzing real-time PCR data by the comparative C(T) method. *Nat Protoc* 3:1101-1108.

Svanborg LM, Hoffman M, Andersson M, Currie F, Kjellin P, Wennerberg A (2010). The effect of hydroxyapatite nanocrystals on early bone formation surrounding dental implants. *Int J Oral Maxillofac Surg* 40:308-315.

Wei S, Kitaura H, Zhou P, Ross FP, Teitelbaum SL (2005). IL-1 mediates TNF-induced osteoclastogenesis. *J Clin Invest* 115:282-290.

Wennerberg A, Albrektsson T (2011). Structural influence from calcium phosphate coatings and its possible effect on enhanced bone integration. *Acta Odontol Scand* 8/31:1-8 [Epub ahead of print].

Wennerberg A, Albrektsson T (2010). On implant surfaces: a review of current knowledge and opinions. *Int J Oral Maxillofac Implants* 25:63-74.

Yonezawa T, Lee JW, Hibino A, Asai M, Hojo H, Cha BY, *et al.* (2011). Harmine promotes osteoblast differentiation through bone morphogenetic protein signaling. *Biochem Biophys Res Commun* 409:260-265.